A Family of Resonant Vibration Control Formats

Krenk, Steen; Høgsberg, Jan Becker

Publication date:
2012

Paper No. 205

A Family of Resonant Vibration Control Formats

Steen KRENK*, Jan HØGSBERG

Department of Mechanical Engineering, Technical University of Denmark
Nils Koppels Alle, Building 403, DK-2800 Kgs. Lyngby, Denmark
sk@mek.dtu.dk, jhg@mek.dtu.dk

ABSTRACT

Resonant control makes use of a controller with a resonance frequency and an equivalent damping ratio. A simple explicit calibration procedure is presented for a family of resonant controllers in which the frequency is tuned to the natural frequency of the targeted mode in such a way that the two resulting modes exhibit identical damping ratio. This tuning is independent of the imposed controller damping. The controller damping is then selected as an optimal compromise between too small damping, and too large damping at which the modal frequencies coincide, and thereby produce undesirable constructive interference. This 'equal modal damping' procedure leads to explicit calibration formulae, and produces a nearly level plateau in the frequency response curve with lower response than the traditional double-root calibration.

Keywords: *Resonant damping, active control, structural vibration.*

1 INTRODUCTION

Resonant vibration control represents a group of control or damping strategies where a resonance in the controller is calibrated specifically with respect to the targeted vibration mode(s) of the structure. When designed and calibrated properly this dedicated control results in effective damping and response mitigation at a limited controller cost. The present paper presents a general resonant vibration control format and a corresponding calibration procedure. The classic resonant control formats are the positive position feedback and the acceleration feedback, where position (strain or extension) or acceleration are measured at the controller location and passed through a resonant second order filter, [1]. For positive position feedback the stiffness is reduced by the controller and the performance is limited by stability when eliminating the stiffness of a particular mode [2], while in acceleration feedback the phase is the opposite of positive position feedback, resulting in unconditional stability. Thus, if the acceleration signal of the low-frequency dynamics can be measured with sufficient by accelerometers, the resonant acceleration feedback format constitutes a robust vibration control method.

The efficiency of resonant control basically requires that the filter frequency of the controller is close to the natural frequency of the structural target mode, and that the filter damping is appropriately balanced to provide the desired dissipation. A calibration procedure for acceleration feedback was presented in [3], in which the choice of unit frequency ratio and critical filter damping leads to design at the cross-over point in the root locus diagram. The performance of the acceleration feedback procedure has subsequently been illustrated e.g. in [4, 5].

The design and calibration of resonant vibration control with position feedback has mainly been developed for piezoelectric transducers [6]. As observed in [7] a piezoelectric transducer shunted with

a suitable electric circuit can generate resonant damping similar to the concept of mechanical vibration absorbers, and in particular the series and parallel RL shunt circuits are commonly applied for passive resonant damping of flexible structures [8, 9]. Various calibration strategies have been presented for these circuits. In [7] the shunt parameters were calibrated with respect to maximum modal damping, resulting in a double root in the associated characteristic equation. Although this leads to large modal damping it also results in constructive interference of the involved modes. Effective vibration reduction can be obtained by designing the shunt circuits with respect to minimum frequency response amplitude [7, 8] or by a fixed-point calibration procedure [10] known from design of the mechanical tuned mass damper [11]. A review of various calibration procedures for RL-circuits has been given in [8]. Piezoelectric transducers are strain (position) based feedback systems, the therefore the robustness and efficiency associated with acceleration feedback control can in principle be obtained by introducing the double time derivative of the acceleration indirectly via the control, as demonstrated in [12] for the so-called negative position feedback. An alternative implementation of resonant acceleration feedback follows from electromagnetic shunt damping, where an electromagnet is coupled to a circuit in which the resonant property is generated via an external capacitance C [13, 14, 15].

The present paper introduces a simple general design procedure for resonant controllers with either acceleration or position feedback. When a controller is introduced to act in resonance with a selected mode, this mode splits into two modes with closely spaced frequencies. By tuning of the resonant controller frequency these closely spaced modes can be given equal damping ratio. When increasing the damping ratio of the resonant controller the modal damping of the two coupled modes increases, while the two frequencies approach each other. The optimal controller damping ratio constitutes a compromise between introducing sufficient modal damping and avoiding constructive interference of the two modes. The optimal design parameters are expressed in simple analytic form using the complex root-locus diagram for an equivalent two-degrees-of-freedom system.

2 RESONANT VIBRATION DAMPING

The principle of resonant vibration control is illustrated in Figure 1, where a control force f_c acts on a structure. The sensor signal $G(\omega)x$ is passed through a resonant filter with frequency ω_c and bandwidth parameter ζ_c, and the frequency characteristics of the actuator are governed by $F(\omega)$.

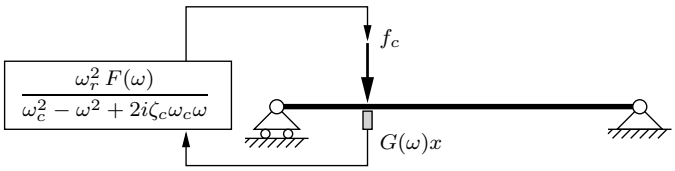

Figure 1: Flexible structure with collocated resonant vibration control.

When $x(t)$ represents a displacement associated with a particular mode r with modal stiffness k_r and modal mass m_r, and a corresponding external load component $f(t)$, the normalized equation of motion for the structure can be written as

$$\ddot{x} + 2\zeta_r\omega_r\dot{x} + \omega_r^2 x \;=\; \omega_r^2\,\frac{f_c + f}{k_r}\,, \tag{1}$$

with the natural frequency $\omega_r \;=\; (k_r/m_r)^{1/2}$ and the damping ratio ζ_r. The resonant controller is described by the second order filter equation presented in Figure 1,

$$\ddot{\xi} + 2\zeta_c\omega_c\dot{\xi} + \omega_c^2\xi \;=\; \omega_r^2 g\,, \tag{2}$$

with control variable $\xi(t)$ and sensor signal $g(t)$. In the frequency domain the control force f_c and the sensor signal g are linear frequency dependent functions of ξ and x, respectively,

$$f_c/k_r \;=\; \alpha F(\omega)\xi, \qquad g \;=\; G(\omega)x. \tag{3}$$

The frequency response relation for this system is

$$x \;=\; \frac{(\omega_c^2 - \omega^2 + 2i\zeta_c\omega_c\omega)\,\omega_r^2}{(\omega_r^2 - \omega^2 + 2i\zeta_r\omega_r\omega)(\omega_c^2 - \omega^2 + 2i\zeta_c\omega_c\omega) - \alpha\omega_r^4 F(\omega)G(\omega)}\,\frac{f}{k_r}. \tag{4}$$

The idea of resonant control is the use of a controller frequency close to the natural system frequency to be controlled, $\omega_c \simeq \omega_r$, whereby the response will be governed by the damping via ζ_r and ζ_c. Substitution of the frequency representation (3) leads to the approximate response at resonance

$$x \;\simeq\; \frac{1}{2i\zeta_{\text{eq}}}\,\frac{f}{k_r} \qquad , \qquad \zeta_{\text{eq}} \;\simeq\; \zeta_r + \frac{\alpha}{4\zeta_c}F(\omega_r)G(\omega_r). \tag{5}$$

This illustrates the basic requirement that $F(\omega_r)G(\omega_r)$ should have a dominating positive real part and that the damping parameter ζ_c must be 'small' for the control to be effective around resonance.

2.1 Root Locus Analysis

The roots of the characteristic polynomial associated with (1) and (2) describe some of the important properties of the combined system, and it has been demonstrated in [16] that the classic frequency response calibration for the mechanical tuned mass damper corresponds to equal modal damping. In the following this pole placement based criteria is used for the calibration of the resonant position and acceleration feedback control formats.

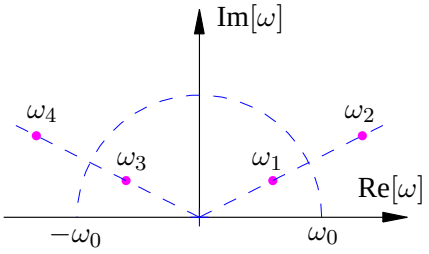

Figure 2: Complex roots ω_1, ω_2 and ω_3, ω_4 as inverse points of circle $|\omega| = \omega_0$.

Let the four roots of a characteristic polynomial be denoted $\omega_1, \cdots, \omega_4$. The corresponding modes have equal damping ratio, if ω_1 and ω_2 lie on the same line containing the origin of the complex plane, as illustrated in Figure 2. This implies that they are inverse points in the complex plane with respect to some real-valued frequency ω_0, i.e.

$$\omega_2/\omega_0 \;=\; \omega_0/\omega_1^*, \tag{6}$$

where ω_1^* denotes the conjugate of ω_1. This reciprocal relation leads to a specific format of the corresponding characteristic polynomial with two parameters χ and λ,

$$\omega^4 \;-\; (2 + 4\chi^2)\,\omega_0^2\omega^2 \;+\; \omega_0^4 \;-\; 4i\lambda\,\chi\omega_0\omega\big(\omega^2 - \omega_0^2\big) \;=\; 0. \tag{7}$$

The property of equal modal damping, as expressed by the inverse root relation (6), is equivalent to imposing a balance in (7) between the cubic and linear terms, so that they cancel at $\omega = \pm\omega_0$.

Root locus diagrams for this particular format are illustrated in Fig. 3. For $\lambda = 0$ there is no damping, and the natural frequencies ω_1 and ω_2 appear as points on the positive real axis. When

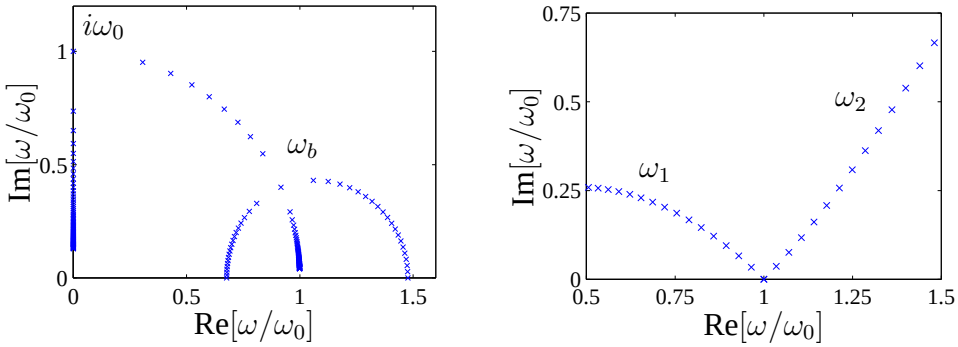

Figure 3: Root locus diagram: (a) $\chi = 0.4$, $\lambda = 0,\ 0.05,\ 0.10\ \cdots$; (b) $\chi = 0,\ 0.05,\ 0.10, \cdots$, $\lambda = \sqrt{2}/2$.

increasing λ for a fixed value of the parameter $\chi < 1$, the roots move into the complex plane as illustrated in Fig. 3a. It follows from the inverse point property, illustrated in Fig. 2, that the two roots ω_1 and ω_2 have equal argument, corresponding to equal damping of the corresponding free modes. This situation changes at the bifurcation point ω_b, which is reached for $\lambda = 1$. The roots then branch off along a circle centered at the origin, with one branch following the circle towards the real axis and the other branch approaching a new branch point on the imaginary axis. In damping of structures the interval of interest is $0 < \lambda \leq 1$. As demonstrated in [16] the special properties of the four roots in Fig. 2 can be used to derive an expression for the damping ratio ζ, and for small values of χ it becomes

$$\zeta \;=\; \frac{\lambda\,\chi}{\frac{1}{2}\big(|\omega_1|/\omega_0 + \omega_0/|\omega_1|\big)} \;\simeq\; \lambda\,\chi. \tag{8}$$

It is seen that damping increases with λ. However, at the bifurcation point constructive interference between the two modes leads to amplification of the response amplitude around resonance, and it follows from the analysis of the mechanical tuned mass damper in [16] that the parameter value $\lambda = \sqrt{2}/2$ is the optimal compromise, where the two roots ω_1 and ω_2 move into the complex plane along curves forming an angle of $\pm 45^\circ$ with the real axis. By (8) this implies the modal damping ratio

$$\zeta \;\simeq\; \tfrac{1}{2}\sqrt{2}\,\chi. \tag{9}$$

In the following, optimal control parameters are determined by identification of the appropriate coefficients of the characteristic polynomial of the control formats with the coefficients in (7).

2.2 Parameter Calibration

The calibration of the filter parameters follows from comparison of the numerator of the frequency response function in (4) with the generic polynomial in (7). For acceleration-position control $\omega_r^2 F(\omega) = \omega_c^2$ and $\omega_r^2 G(\omega) = \omega^2$, [17]. Upon elimination of the reference frequency ω_0 it is found that

$$\omega_c \;=\; \omega_r. \tag{10}$$

The filter damping is subsequently identified by comparison of both the quadratic and cubic terms, and upon elimination of χ this gives

$$\zeta_c^2 \;=\; \tfrac{1}{2}\alpha. \tag{11}$$

There is a simple and important relation between the modal damping ratio ζ of the controlled modes and the damping ratio ζ_c of the controller. In the present case

$$\zeta \;\simeq\; \tfrac{1}{2}\zeta_c. \tag{12}$$

This result permits explicit design of the controller from the desired modal damping ratio. Similar results apply to the other resonant controller formats as discussed in relation to multi-degree-of-freedom systems next.

3 DESIGN OF CONTROL FORMATS

The calibration of four (single gain) resonant control formats is summarized in this section. For a single collocated sensor/actuator pair acting on a MDOF structure the frequency equation of motion is

$$\big(-\omega^2 \mathbf{M} + i\omega \mathbf{D} + \mathbf{K} \big) \mathbf{x} \;=\; \mathbf{w} f_c + \mathbf{f} \,, \tag{13}$$

where the scalar control force is represented in terms of the frequency transfer function $F(\omega)$ as

$$f_c \;=\; \beta \, F(\omega) \, \xi \,, \tag{14}$$

and the corresponding resonant control equation is

$$\big(-\omega^2 + 2i\zeta_c \omega_c \omega + \omega_c^2 \big) \xi \;=\; G(\omega) \mathbf{w}^T \mathbf{x}. \tag{15}$$

In the above expressions β is the scalar gain parameter, while the connectivity array reduces to a column vector **w** in the case of a single transducer. The calibration of the various resonant control formats is based on the free vibration characteristics of the structure. The controller is targeted at mode r with mode shape vector $\mathbf{u}_r$ normalized to unit modal mass. The calibration is based on a single-mode representation of the response,

$$\mathbf{x} \;=\; \mathbf{u}_r x_r, \tag{16}$$

where x_r is the modal coordinate. Substitution of (16) into both (13) and (15), followed by pre-multiplication of (13) with $\mathbf{u}_r^T$, gives the scalar structural equation

$$\big(-\omega^2 + 2i\zeta_r \omega_r \omega + \omega_r^2 \big) x_r \;=\; \nu_r \beta F(\omega) \, \xi \,, \tag{17}$$

and the control equation

$$\big(-\omega^2 + 2i\zeta_c \omega_c \omega + \omega_c^2 \big) \xi \;=\; \nu_r G(\omega) x_r \,. \tag{18}$$

The parameter $\nu_r \;=\; \mathbf{w}^T \mathbf{u}_r$ represents the modal amplitude of the structure at the sensor/actuator location, and may for all formats be absorbed by the gain parameter as $\alpha \;=\; \nu_r^2 \beta$. Four resonant control formats are summarized and characterized in Table 1 in terms of $G(\omega)$ and $F(\omega)$, where the acceleration-position format discussed in Section 2.2 appears as the first case. The last column gives the stability limit, discussed in detail in [18].

Table 1: Frequency functions and stability limit for resonant control formats.

Control format	$G(\omega)$	$F(\omega)$	β_{stab}
Acceleration	ω^2	ω_c^2	∞
Extended acceleration	ω^2	$\omega_c^2 + 2i\zeta_c\omega_c\omega$	∞
Position	ω_r^2	ω_c^2	$\big(\mathbf{w}^T\mathbf{K}^{-1}\mathbf{w}\big)^{-1}/\omega_r^2$
Extended position	ω_r^2	$\omega_c^2 + 2i\zeta_c\omega_c\omega$	$\big(\mathbf{w}^T\mathbf{K}^{-1}\mathbf{w}\big)^{-1}/\omega_r^2$

The calibration of the four control formats is based on direct comparison of the characteristic equation with the generic equation (7), as discussed in Section 2.2. The results are summarized in Table 2, where the first row corresponds to (10)-(12).

Frequency curves for the dynamic amplification of an ideal SDOF structure are shown for the four control formats in Figure 4. The dotted curves, corresponding to integer powers of ω, indicate the inclination of the plateau around resonance. It is seen that the additional derivative in the extended formats is able to reduce the inclination compared to the corresponding simple feedback format.

Table 2: Resonant control parameters.

Feedback format	ω_c	ζ_c	ζ
Acceleration	ω_r	$\sqrt{\frac{1}{2}\alpha}$	$\frac{1}{2}\zeta_c$
Extended Acceleration	$\omega_r/(1+\alpha)$	$\sqrt{\frac{1}{2}\alpha/(1+\alpha)}$	$\frac{1}{2}\zeta_c\sqrt{1+\alpha}$
Position	$\omega_r/\sqrt{1-\alpha}$	$\sqrt{\frac{1}{2}\alpha}$	$\frac{1}{2}\zeta_c/\sqrt{1-\alpha}$
Extended position	$\omega_r\sqrt{1-\alpha}$	$\sqrt{\frac{1}{2}\alpha/(1-\alpha)}$	$\frac{1}{2}\zeta_c$

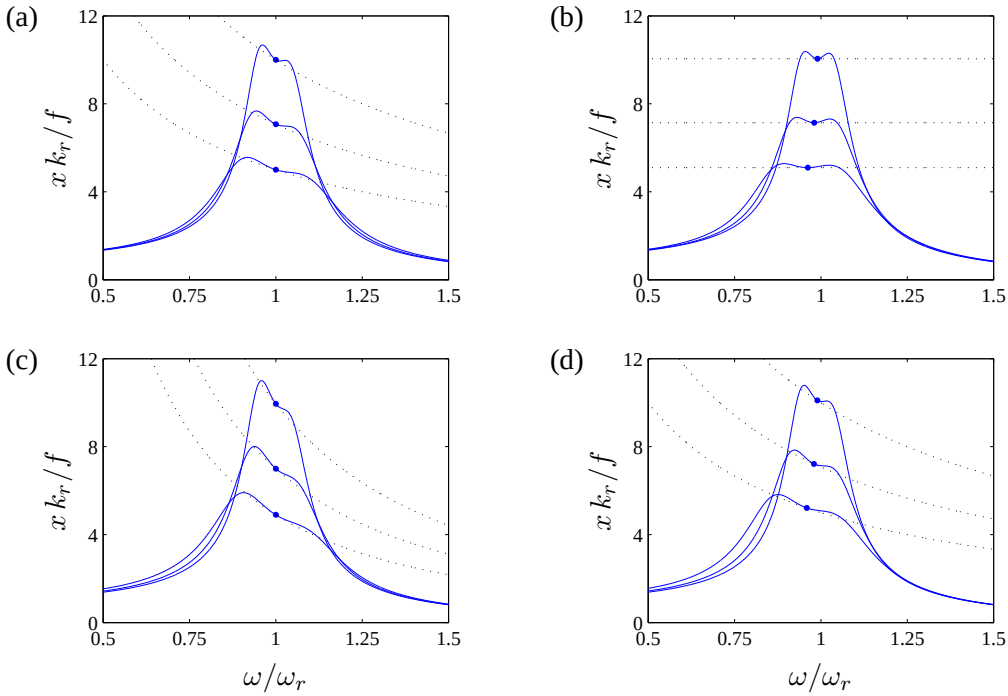

Figure 4: Dynamic amplification factor: (a) velocity, (b) extended acceleration, (c) position, (d) extended position feedback. Gain parameter $\alpha = 0.02$, 0.04 and 0.08.

The performance of resonant vibration control when acting on a flexible structure is in this case illustrated for a transducer acting on a simply supported beam, as shown in Figure 1. The beam is modelled by 10 Bernoulli Euler beam elements of equal length, and the controller/actuator are located at a distance from the support $a/\ell = 0.5$ or 0.2, where the latter location implies reduced authority compared to the former. Numerical results are presented for acceleration feedback with parameters as described in the first rows in Tables 1 and 2. Figures 5(a,c) show the root locus curves for the present calibration (solid) and the double root calibration (dashed) from e.g. [7, 8]. The damping ratio $\zeta = \mathrm{Im}[\omega/|\omega|$ is shown in Figs. 5(b,d). It is seen that equal modal damping is attained to great accuracy by the present calibration procedure at $a/\ell = 0.5$, and also with fairly good accuracy in the case of the indirect control at $a/\ell = 0.2$, while double-root calibration is less robust as well as less efficient due to constructive mode interference.

The dynamic amplification of the harmonic response at the center of the beam is shown in Figure 6(a,c). The transverse load is uniformly distributed over the entire span of the beam. It is seen that the present calibration procedure effectively reduces the response amplitude, while for the double root calibration the closely spaced poles result in amplification of the response around resonance. The amplitude of the control force is shown in Figs. 6(b,d), which indicates that the improved per-

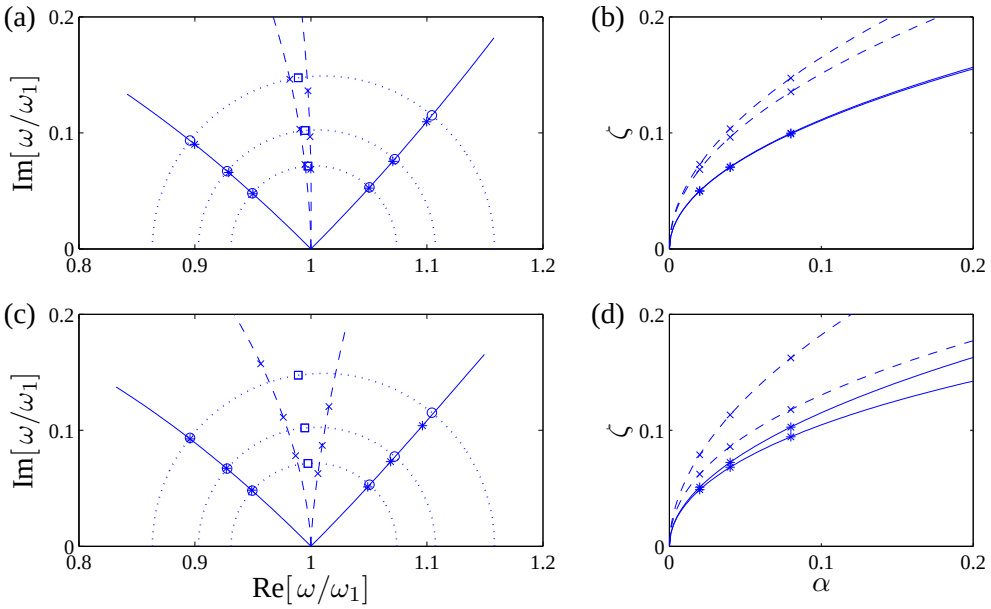

Figure 5: Acceleration feedback: Root locus (a,c) and modal damping (b,d) for $a/\ell = 0.5$ (a,b) and 0.2 (c,d).

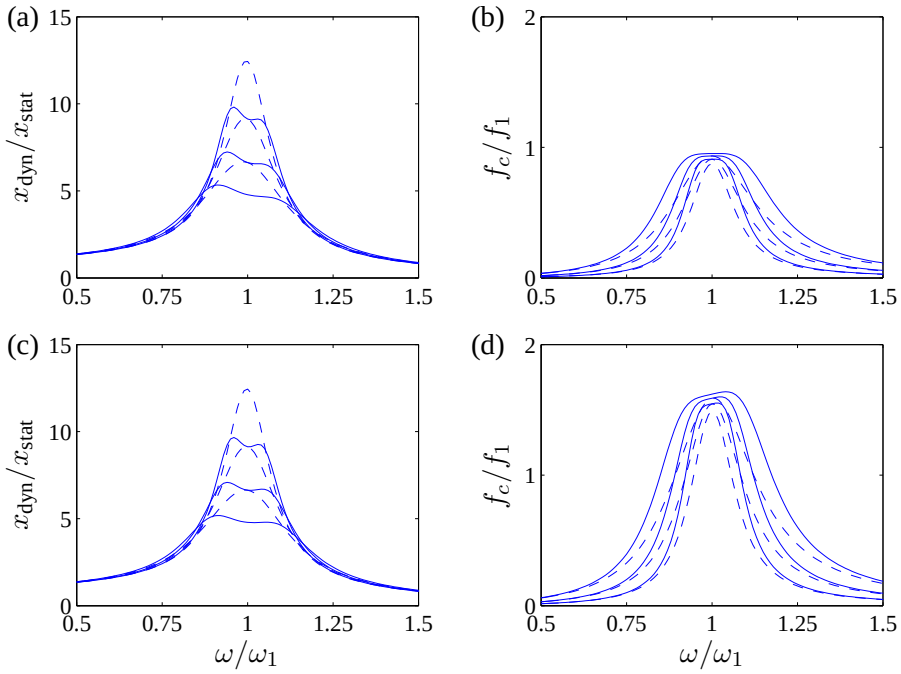

Figure 6: Acceleration feedback: Displacement (a,c) and control force (b,d) amplitudes for $a/\ell = 0.5$ (a,b) and 0.2 (c,d).

formance of the present calibration results in a slightly larger bandwidth compared to the double-root calibration.

4 CONCLUSIONS

A design procedure has been presented for calibration of collocated resonant control of structures. The is based on equal modal damping ratio of the two modes generated via interference of the targeted mode and the controller. A key point is the separation of the frequencies of these modes whereby better effect than for the more classic double-root calibration is attained. The procedure is described in more detail in [18]. When used in connection with flexible structures the influence of the flexibility from non-targeted high-frequency vibration modes can be taken into account by a quasi-

static correction of the sensor signal. This leads to modified calibration expressions, as demonstrated in [19, 20, 21].

REFERENCES

[1] Preumont, A. (2002) *Vibration Control of Active Structures. An Introduction,* 2nd ed., Kluwer, Dordrecht, The Netherlands.

[2] Fanson, J.L. & Caughey, T.K. (1990) Positive position feedback control for large space structures, *AIAA Journal*, 28(4):717–724.

[3] Goh, C.J. & Yan W.Y. (1996) Approximate pole placement for acceleration feedback control of flexible structures, *Journal of Guidance, Control, and Dynamics*, 19:256–259.

[4] de Noyer, M.P.B. & Hanagud, S.V. (1998) Single actuator and multi-mode acceleration feedback control, *Journal of Intelligent Material Systems and Structures*, 9(7):522–533.

[5] Kim, S.-M., Pietrzko, S. & Brennan, M.J. (2008) Active vibration isolation using an electrical damper or an electrical dynamic absorber, *IEEE Transactions on Control Systems Technology*, 16:245–254.

[6] Moheimani, S.O.R. (2003) A survey of recent innovations in vibration damping and control using shunted piezoelectric transducers, *IEEE Transactions on Control Systems Technology* 11:482–494.

[7] Hagood, N.W. & von Flotow, A. (1991) Damping of structural vibrations with piezoelectric materials and passive electrical networks. *Journal of Sound and Vibration*, 146:243–268.

[8] Caruso, G. (2001) A critical analysis of electric shunt circuits employed in piezoelectric passive vibration damping, *Smart Materials and Structures*, 10:1059–1068.

[9] Preumont, A., de Marneffe, B., Deraemaeker, A. & Bossens, F. (2008) The damping of a truss structure with a piezoelectric transducer, *Computers and Structures*, 86:227–239.

[10] Yamada, K., Matsuhisa, H., Utsuno, H. & Sawada, K. (2010) Optimum tuning of series and parallel LR circuits for passive vibration suppression using piezoelectric elements, *Journal of Sound and Vibration*, 329:5036–5057.

[11] Den Hartog, J.P. (1956) *Mechanical Vibrations*, 4th ed., McGraw-Hill, New York.

[12] Kim, S.-M., Wang. S. & Brennan, M.J. (2011) Comparison of negative and positive position feedbck control of a flexible structure. *Smart Materials and Structures*, 20:015011 (10pp).

[13] Behrens, S., Fleming, A.J. & Moheimani, S.O.R. (2005) Passive vibration control via electromagnetic shunt damping, *IEEE/ASME Transactions on Mechatronics*, 10(1):118–122.

[14] Inoue, T., Ishida, Y. & Sumi, M. (2008) Vibration suppression using electromagnetic resonant shunt damper, *Journal of Vibration and Acoustics*, 130:041003 (8pp).

[15] Cheng, T.-H. & Oh, I.-K. (2009) A current-flowing electromagnetic shunt damper for multi-mode vibration control of cantilever beams, *Smart Materials and Structures*, 18:095036 (10pp).

[16] Krenk, S. (2005) Frequency analysis of the tuned mass damper, *Journal of Applied Mechanics ASME*, 72:936–942.

[17] Sim, E. & Lee, S.W. (1993), Active vibration control of flexible structures with acceleration feedback, *Journal of Guidance, Control, and Dynamics*, 16:413–415.

[18] Krenk, S. & Høgsberg, J. (2012) Equal modal damping design for a family of resonant control formats. Technical University of Denamrk, (to be published).

[19] Krenk, S. & Høgsberg, J. (2009) Optimal resonant control of flexible structures. *Journal of Sound and Vibration*, 323:530–554.

[20] Svendsen, M.N., Krenk, S. & Høgsberg, J. (2011) Resonant vibration control of rotating beams. *Journal of Sound and Vibration*, 330:1877–1890.

[21] Krenk, S., Svendsen, M.N. & Høgsberg, J. (2012) Resonant vibration control of three-bladed wind turbine rotors, *AIAA Journal*, 50(1):148–161.